



Nonlinear analysis of tunnel slab under hydrogen explosion

Lui, W., Markert, F., Shentsov, V., & Giuliani, L. (2023). *Nonlinear analysis of tunnel slab under hydrogen explosion*. Paper presented at 10th International Symposium on Tunnel Safety and Security, Stavanger, Norway.

[Link to publication record in Ulster University Research Portal](#)

Publication Status:

Published (in print/issue): 26/04/2023

Document Version

Author Accepted version

General rights

Copyright for the publications made accessible via Ulster University's Research Portal is retained by the author(s) and / or other copyright owners and it is a condition of accessing these publications that users recognise and abide by the legal requirements associated with these rights.

Take down policy

The Research Portal is Ulster University's institutional repository that provides access to Ulster's research outputs. Every effort has been made to ensure that content in the Research Portal does not infringe any person's rights, or applicable UK laws. If you discover content in the Research Portal that you believe breaches copyright or violates any law, please contact pure-support@ulster.ac.uk.

Nonlinear analysis of a tunnel slab under a hydrogen explosion

Wenqian Liu¹, Frank Markert¹, Volodymyr Shentsov² & Luisa Giuliani¹

¹Technical University of Denmark, Lyngby, Denmark

²Ulster University, Newtownabbey, United Kingdom

ABSTRACT

Hydrogen explosions consequent to hydrogen-fuelled vehicle (HFV) accidents in a tunnel could cause great losses of lives and property due to its special characteristics, such as high pressure blast waves. Reliable predictions on the structural response of a tunnel impacted by blast waves are crucial to develop effective mitigation technologies to protect the integrity of the structure. This case study conducts a numerical analysis of a tunnel ventilation slab subjected to an explosion wave calculated by a CFD study on this specific scenario. The focus here is the mechanical structural response of a reinforced concrete (RC) slab caused by the pressure time history of the explosion wave in the case tunnel. Two different finite element codes (ANSYS Mechanical APDL and DIANA) are applied comparing the respective results. The effects of the reinforcement diameter, reinforcement position, concrete strength and boundary condition are studied and discussed. Numerical results show that the RC slab suffers significant damage under larger explosive impulses. The influences of reinforcement position and concrete strength on the RC slab deflection are very slight. However, reinforcement diameter and boundary condition play an essential role in the RC slab dynamic response. Improving reinforcement diameter and reducing the freedom of the RC slab can effectively enhance the properties of the RC ventilation slab under hydrogen explosion loads.

KEYWORD: reinforcement concrete, tunnel ventilation slab, hydrogen tank explosion, numerical simulation, parametric analysis

1. INTRODUCTION

1.1 Background

Tunnels are essential infrastructures that can provide a cost-effective solution to direct transport between two locations, e.g., separated by mountains, water, or heavily populated areas of urban cities. However, a tunnel structure may be heavily damaged in case of a severe explosion accident. The resulting pressure time history of the explosion wave inside the tunnel is more severe than comparable explosions in unconfined and/or uncongested environments as in open space due to the close-in effects in the tunnel [1]. For example, a methane explosion that occurred in Qishanyan (QSY) tunnel in China caused the tunnel to collapse and trapped 12 workers [2]. In 2020, a mountain tunnel in Turkey collapsed due to an explosion caused by a gas leak, leading to 11 casualties [3]. In view of the consequences of tunnel accidents, it is crucial to study structural performance under explosion conditions to avoid structure collapse and reduce the potential hazards to public safety.

The main role of the tunnel is to provide normal and safe operation of transport. With the promotion of renewable energy, hydrogen vehicles are expected to be a common transport technology. Compared with conventional vehicles, the hazards from hydrogen vehicle accidents are somewhat different and may include gas explosion scenarios. An initial hydrogen leakage is expected to result in a hydrogen jet fire or hydrogen gas cloud explosion depending on the ignition time. An external fire could lead to a hydrogen gas tank rupture in case the safety valve provided with any hydrogen pressure tank is

malfunctioning. In light of LaFleur's risk assessment of hydrogen vehicle accidents [4], the highest risk is the hydrogen tank rupture resulting in a blast wave and a fireball. A hydrogen explosion can lead to extremely dangerous impacts due to high energy and overpressure. Nevertheless, the probability of a tank rupture causing a blast wave in a hydrogen vehicle accident is very low (about 0.092%) [5, 6]. As explained before, the severeness of hydrogen explosions in a tunnel is more dangerous than that in the opening surrounding [7], because the explosive wave diameter is possibly larger than the tunnel height or width, and the explosive wave can impinge on the tunnel structure surface [8].

Presently, experimental and numerical analysis are two popular methods to predict the structural dynamic behaviour under explosions. However, owing to the complicated and expensive explosion experiment in a tunnel, FE (finite element) analysis is a preferred tool to investigate the nonlinear dynamic response of the structure.

For example, Senpei Wang et al. [9] investigated the reinforcement concrete (RC) structures' response under gas explosions using LS-DYNA based on different parameters, such as concrete compressive strength, reinforcement strength, and section type. The results showed that the RC response is dominated by the tensile membrane determined by the reinforcement steel strength, and different section types lead to different RC responses. M. Buonsanti et al. [10] performed the dynamic response of tunnel walls defining a liquefied petroleum gas (LPG) explosion by adopting ANSYS code, which illustrated that the position of the primary displacement is where the instantaneous impact is. Zhipeng Li et al. [11] studied the dynamic response and damage process of the concrete lining in the tunnel in line with the explosion wave by using LS-DYNA. Their results indicate that the maximum displacement is in 5m of the detonation site region, and the local damage zone developed along the longitudinal and circumferential directions of the concrete lining.

With reference to previous research [12-15], most of the work is concentrated on the explosion of the tunnel's main structure other than the secondary structures (i.e., a ventilation slab or a smoke duct slab in a tunnel ventilation scheme). And yet secondary structures are easier to collapse under internal tunnel explosion scenarios because of the shortage of supports from surrounding rock or soil mass [16]. In addition, the internal tunnel explosion mainly focuses on typical fuel explosions, e.g., TNT, natural gas, methane, and LPG gas. However, hydrogen is gradually expected to be used in vehicles as an alternate fuel, and the hydrogen tank rupture from a vehicle's fire is more hazardous than other common fuels due to the expected high explosion pressures. Therefore, to present the characterizing hazards of an explosion from a tank filled with hydrogen in the tunnel, the ventilation slab dynamic response to a hydrogen tank explosion will be investigated in this study.

1.2 Purpose and method

In terms of tunnel structural design, many types of secondary structures are found in a tunnel. In the present case study conducted within the HyTunnel CS project [17], a ventilation slab is chosen as the structure to be investigated. The aim of this study is to investigate if and to what extent a hydrogen tank blast could affect the integrity and functionality of the RC tunnel ventilation slab. Hence, this work first analyses the influence of the hydrogen tank blast impulse on the RC slab and then analyses the effects of different parameters on the RC dynamic response under the hydrogen tank rupture due to external fire. These parameters contain reinforcement diameter, reinforcement position, concrete strength, and RC slab boundary conditions. All analyses are carried out both in ANSYS Mechanical APDL and DIANA, and deflection response results are compared with some standards to forecast if the slab will collapse.

2. IMPLEMENTATION OF FE MODELS

2.1 Concrete material model

An appropriate model of the concrete material, including nonlinear behavior, softening, and cracking, is essential to model the collapse of a concrete element under exceptional loads is of interest. Herein,

the concrete compressive and tensile softening material models implemented in ANSYS and DIANA are the basis.

The ANSYS Mechanical APDL software provides the exponential HSD [18] (hardening, softening, and dilatation) model with Drucker-Prager concrete surface failure (HSD2-DP). This model is therefore used for the concrete material. The HSD2-DP model defines concrete tensile fracture energy, tensile and compressive dilatancy, and compressive and tensile strength. In the DIANA software, a Multi-linear curve model is selected to model the concrete compressive behavior together with the Hordijk tensile model [19] for concrete tensile response modeling. Comparing the stress-strain performance in both software, the Multi-linear curve in DIANA adopts the same stress-strain value of ANSYS. The tensile fracture energy value is defined the same in HSD2 and Hordijk models. Concrete compressive and tensile models in two software can be found in Figure 1.

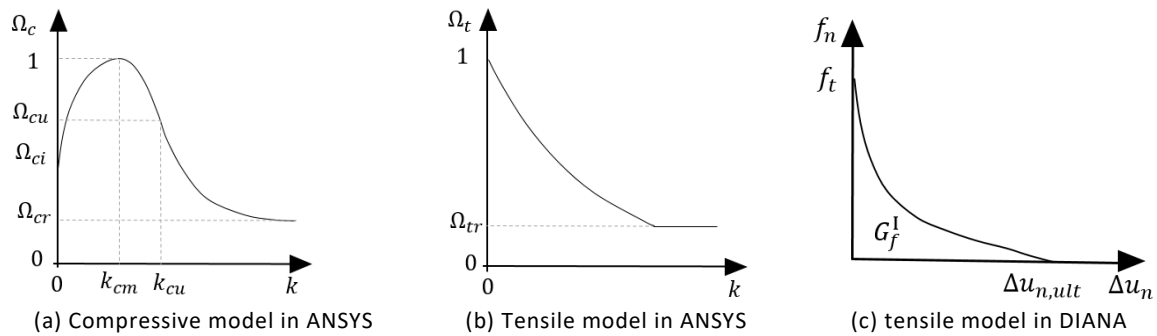


Figure 1 Concrete material model in ANSYS and DIANA [18, 19]

In Figure 1, Ω_c and Ω_t are the hardening and softening behavior of concrete yield surfaces, k_{cu} is the plastic strain at the transition from power law to exponential softening, k_{cm} is the plastic strain at uniaxial compressive strength, Ω_{ci} is relative stress at start of nonlinear hardening, Ω_{cu} is residual relative stress at k_{cu} , Ω_{cr} is the residual compressive relative stress, Ω_{tr} is the residual tensile relative stress, G_f^I is concrete tensile fracture energy, $\Delta u_{n,ult}$ is concrete crack width, f_t is concrete tensile strength. In this paper, $\Omega_{cr} = 0.1$, $\Omega_{ci} = 0.4$, $\Omega_{cu} = 0.7$, $k_{cm} = 0.003 - f_c/E_c$, $k_{cu} = 0.0045 - f_c/E_c$, $\Omega_{tr} = 0.01$, where f_c is the concrete compressive strength, E_c is the concrete elastic modulus.

2.2 Steel material model

In both software, steel yield strength, elastic modulus, and ultimate strain adopt the same values. The difference between the two software is the steel material model. In particular, the Multi-linear Kinematic Hardening model is chosen for defining the steel stress-strain curve in ANSYS, while the Von Mises plasticity with plastic strain-yield stress is used in DIANA[20].

2.3 Strain rate effect

The strain rate effect has an essential role in concrete structural dynamic behavior, resulting in material mechanical properties always being different from static loading when concrete structures suffer impacts from explosion waves [21]. Plenty of research indicated that higher strain rates result in higher strength and brittle failure processes [22, 23]. In order to show the material strength increase under a high strain rate, the dynamic increase factor (DIF) is applied to depict the relationship among the static strength, strain rate, and dynamic strength. In this study, DIFs of concrete compressive and tensile strength adopt expressions from CEB [24].

$$DIF_c = \begin{cases} \frac{f_{cd}}{f_c} = \left(\frac{\dot{\varepsilon}_c}{\dot{\varepsilon}_{c0}}\right)^{1.026\alpha_s} & \text{for } |\dot{\varepsilon}_c| \leq 30s^{-1} \\ \frac{f_{cd}}{f_c} = \gamma_s \left(\frac{\dot{\varepsilon}_c}{\dot{\varepsilon}_{c0}}\right)^{\frac{1}{3}} & \text{for } |\dot{\varepsilon}_c| > 30s^{-1} \end{cases} \quad (1)$$

$$DIF_t = \begin{cases} \frac{f_{td}}{f_t} = \left(\frac{\dot{\varepsilon}_t}{\dot{\varepsilon}_{t0}}\right)^{1.0165\delta_s} & \text{for } |\dot{\varepsilon}_t| \leq 30s^{-1} \\ \frac{f_{td}}{f_t} = \beta_s \left(\frac{\dot{\varepsilon}_t}{\dot{\varepsilon}_{t0}}\right)^{\frac{1}{3}} & \text{for } |\dot{\varepsilon}_t| > 30s^{-1} \end{cases} \quad (2)$$

$$\alpha_s = \frac{1}{5 + \frac{9f_c}{f_{c0}}} \quad (3)$$

$$\log \gamma_s = 6.156\alpha_s - 2 \quad (4)$$

$$\delta_s = \frac{1}{10 + \frac{6f_c}{f_{c0}}} \quad (5)$$

$$\log \beta_s = 7.112\delta_s - 2.33 \quad (6)$$

Where f_{cd} is the concrete dynamic compressive strength, $\dot{\varepsilon}_c$ is the compressive strain rate, $\dot{\varepsilon}_{c0} = -30 \times 10^{-6} s^{-1}$, α_s is the coefficient, f_{c0} is constant and equal to 10MPa, γ_s is the coefficient, f_{td} is the concrete dynamic tensile strength, f_t is the concrete static tensile strength, $\dot{\varepsilon}_t$ is the tensile strain rate, $\dot{\varepsilon}_{t0} = 3 \times 10^{-6} s^{-1}$, δ_s and β_s are coefficients [24].

For the steel bars model, the DIF expression (Eq. (7) and (8)) from Malvar and Crawford[25] is used in this study, where $\dot{\varepsilon}$ is the strain rate, and f_y is steel static yield stress.

$$DIF = \left(\frac{\dot{\varepsilon}}{10^{-4}}\right)^\alpha \quad (7)$$

$$\alpha = 0.074 - 0.04 \frac{f_y}{414} \quad (8)$$

3 VALIDATION OF THE FE MODEL

3.1 Test study introduction

To validate the dynamic model of an RC structure that suffered an explosion, a simpler model of an RC beam studied in literature was first implemented and simulation results were compared with experimental data reported in Bin Rao [26]. The RC. beam was tested with a 13.4kg TNT charge and 1.5 m stand-off distance. The cylindrical explosive was detonated at both ends. The beam was 2.5 m long and had a squared section with 0.2 m side. The concrete was C40 grade and the steel of the longitudinal steel bars was HRB 335, having a yield strength of 466.7MPa.

The RC beam has four 20mm longitudinal bars and average spacing of 150mm for 8mm stirrups. The tested beam was placed in a hole, so that the upper surface of a beam was level with the ground surface. Four rectangular steel plates and nuts are used to constrain the tested beam. In the interest of obtaining the explosive pressure on the beam, three pressure transducers were set parallel to the upper surface of a beam in this test. Furthermore, three displacement transducers were arranged on the tested beam bottom surface to detect the beam deflection response.

3.2 FE models in software

The external explosion pressure wave impact on the structure varies significantly along the structure surface and with time. Thus, it is challenging to map each resulting point pressure of the structure when analyzing the explosive behavior. To simplify the external surface load pattern, uneven loads have been

divided into several uniform loads along the structure element surface, as shown in Figure 2. In this FE model, the explosive pressure was then simplified according to the test pressure position of sensors. Thus, the external load is predicted assuming that the overpressure is uniform between the half distance of the adjacent pressure sensors, and the pressure-time curve adopts the central pressure sensors value, as shown in Table 1.

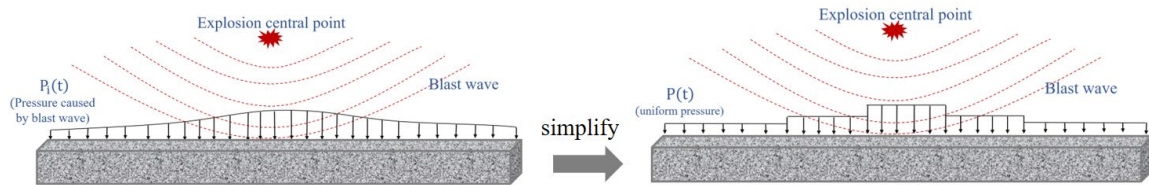
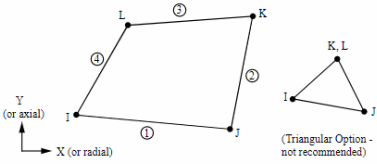
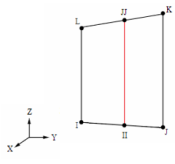
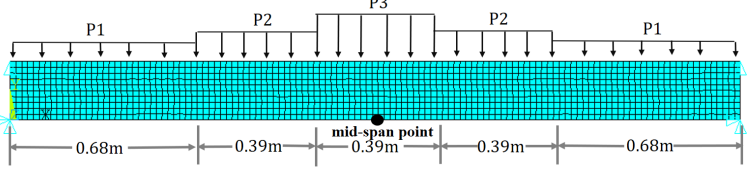
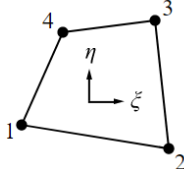
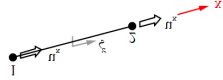
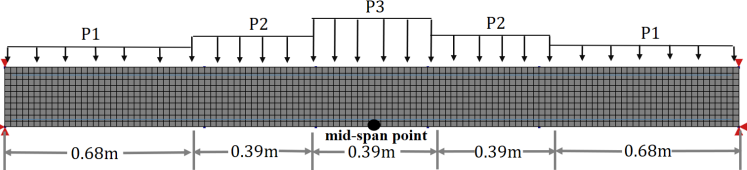


Figure 2 Explosive loads transformation diagram

Table 1 FE models in ANSYS and DIANA

Software	Concrete	Reinforcement	Mesh size(m)
ANSYS	<p>Element type: PLANE 182</p> 	<p>Element type: REINF 263</p> 	0.02
			
	<p>Element type: Q8MEM</p> 	<p>Element type: L2TRU</p> 	0.02
			

To improve the calculation efficiency and reduce the simulation errors, the FE model was simplified to a 2D model with various uniform pressure. The respective 2D FE model in ANSYS and DIANA are summarized in Table 1. In ANSYS, the concrete is simulated by the PLANE182 element, a four-node element with two degrees at each node. And the reinforcing steel is simulated by the REINF263 element, a two-node element with two degrees of freedom at each node. It is worth noting that REINF263 uses a smeared approach and is defined by a mesh-independent method. In DIANA, the concrete uses a Q8MEM element with four nodes, and steel bars use an L2TRU element with two nodes. For both the FE software, reinforcements are embedded in the concrete and their element sizes are 0.02m.

Notably, the pressure unit is different in ANSYS and DIANA, and the actual input external force should be transformed into new data based on the real surface overpressure. For example, the explosion is applied on the top line of the 2D FE model, and this force is still a pressure which units is MPa in ANSYS when using PLANE182 element. But the line pressure unit is N/m in DIANA. Notably, the line pressure in DIANA is obtained by multiplying the real area pressure and the beam width.

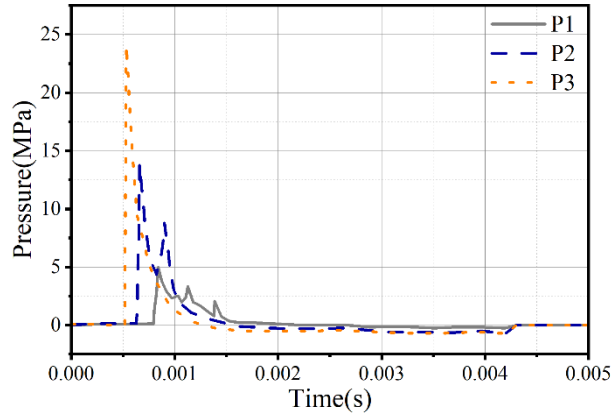


Figure 3 Input external force[26]

In Table 1, P1, P2 and P3 can be found in Figure 3, and P1 is in the beam central part with large peak pressure. The external loads of the RC beam in Figure 3 are from TNT explosion[26]. The mid-span point is the deflection measured point in both software, and this point is in the middle of the bottom surface. Two nodes in the beam bottom surface are fixed in vertical and horizontal directions, and another two in the beam top surface are only fixed in vertical directions, as shown in. Table 1.

3.3 Comparison of FE results and test data

Figure 4 presents the x-component strain of the RC beam under the last time step in ANSYS. In that element strain contours, the elastic phase of the beam is from -0.000598 to 0.0000984, while other ranges indicate concrete cracking. The positive strain value means the beam is in tension and the negative strain value is the compression. It is worth noting that most of the concrete area is cracking due to tensile failure, only a few part closed to the support is still in elastic after the TNT blast.

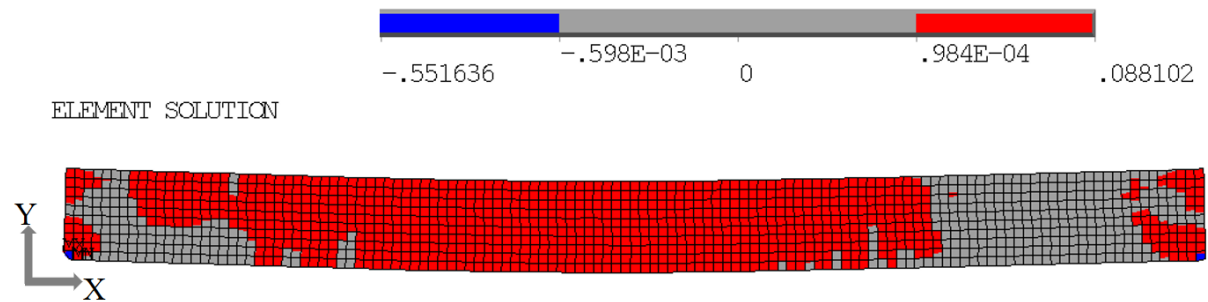


Figure 4 Concrete element failure diagram in ANSYS (X-component strain)

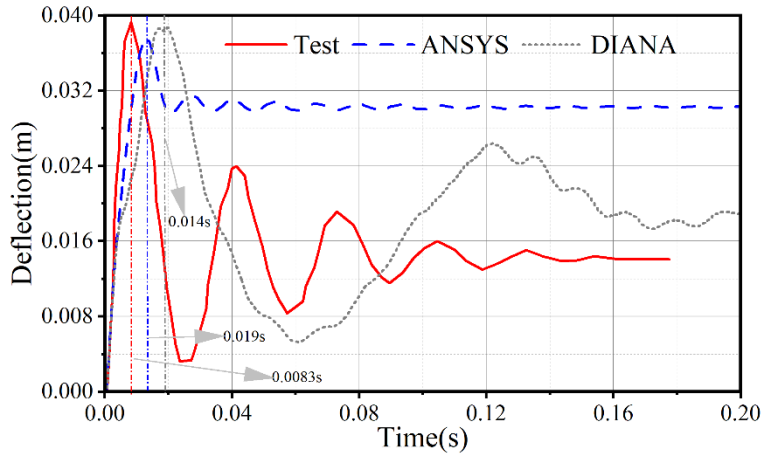


Figure 5 Comparison of RC beam mid-span deflection response with the test [26]

To validate FE models, deflection time histories extracted from a mid-span point are compared with the test data. Following simulation results from ANSYS and DIANA, deflection responses are shown in Figure 5. It can be seen from Figure 5 that the maximum deflection value in both software is very similar, namely 0.04m in test, 0.037m in ANSYS and 0.0385m in DIANA. Thus, for the peak deflection of the RC beam, the FE models using ANSYS and DIANA compare well and are regarded valid to be applied in the following.

4. FE MODELING OF THE TUNNEL SLAB

4.1 FE model dimension and boundary

On the basis of the background of the HyTunnel CS project [17], the dynamic performance of an RC tunnel ventilation slab is explored in this paper. In this study case, the RC tunnel ventilation slab suffered a pressure wave due to the explosion of a hydrogen tank of 62.4L and 700 bar, with a total mass of 2.5kg in a tunnel with a cross-section area of 83m². This study adopts the hydrogen explosion force obtained through a CFD analysis of a tunnel involved in the HyTunnel CS project [17], the validated against experiments CFD model that was employed for simulation of blast wave is based on [27] The pressure curve has 2 distinct peaks, the first one is leading shock that first touches the ceiling at 0.01 s and the second is reflected from walls and focusing at the middle of the ceiling hence increased by 50 kPa at 0.015 s.

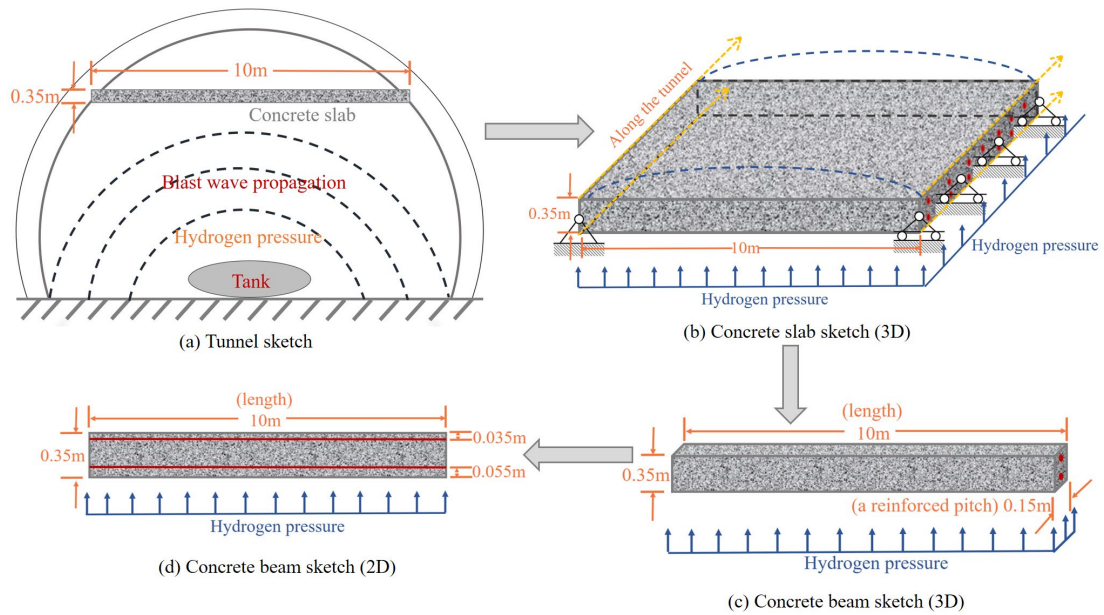


Figure 6 2D model simplified process

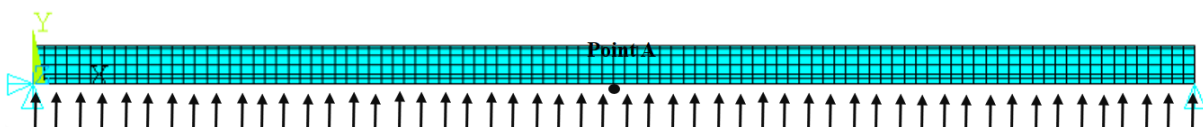
The RC ventilation slab in a tunnel is simplified to a supported 2D RC beam, as shown in Figure 6. This is because the RC ventilation slab is a simply supported slab along a longitudinal direction of a tunnel, which caused consistent deformation of the whole slab when it suffered external force. Another main reason not mentioned is that the action considered does not vary along the length (most critical point). Based on these assumptions, the problem is planar and can be adequately represented in two dimensions and use of 3D model is less favourable in terms of computational efforts.

In this RC slab, a section of a spaced (150mm) longitudinal bar is extracted to form a simply supported beam with two steel bars. One bar is in the tensile zone; another bar is in the compressive zone. The length of the RC slab is 10m, and the height is 0.35m. It is worth noting that the force from the point that suffered the largest explosion is assumed to apply uniformly to the concrete slab. This is a simplification due to the fact that the maximum pressure recorded at the ceiling above the tank explosion location to account for the conservative estimation of the slab reaction in FEM analysis. As been previously show in [28] the series of blast waves are produced after explosion resulting in reflections and focusing. Authors aware of the physics behind and take this simplifications into account due to difficulty in realisation without two way coupling of CFD and FEM.

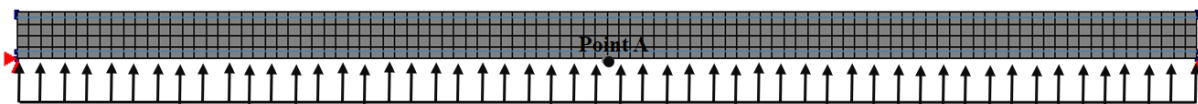
Line with the parameters of the concrete slab in the tunnel, Table 2 refers to the fundamental dimension of the 2D simplified supported beam. The concrete grade is C35, and the reinforcing steel is class C with a yield strength 500MPa. The FE model in ANSYS and DIANA can be found in Figure 7. Two nodes on the beam edges are constrained in these two FE models. One node is fixed in a horizontal and vertical direction; another node is only fixed in a vertical direction. The element mesh size of both FE models is 0.5m. The deflection response detected point is point A in two FE models, as shown in Figure 7.

Table 2 Basic information of the concrete beam model[17]

Dimension of concrete beam			Concrete cover(m)		Steel bar	
Width(m)	Length(m)	Height(m)	tensile zone	compressive zone	No. bar	Diameter
0.15	10	0.35	0.035	0.055	2	0.016



(a) FE model in ANSYS



(b) FE model in DIANA

Figure 7 FE models in ANSYS and DIANA

4.2 Response of the slab under hydrogen explosion

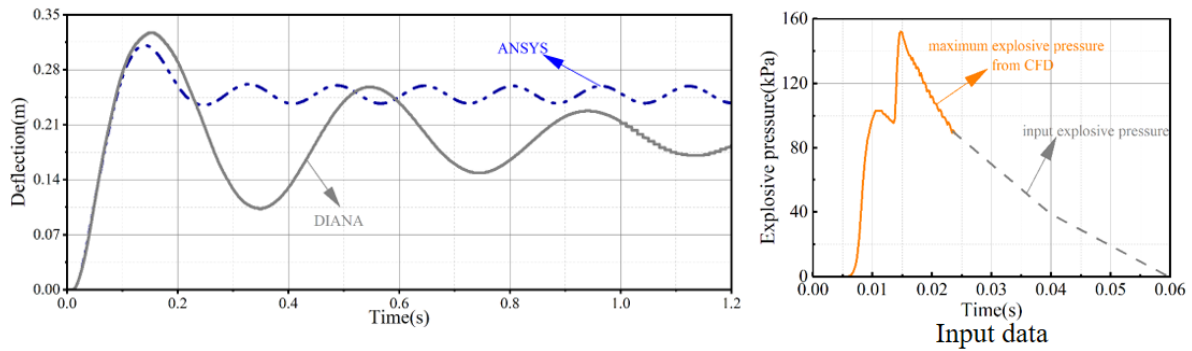
According to the input pressure [17], the duration (0.024s) of the pressure impact caused by the hydrogen explosion) is shorter than the beam natural period (0.17s), which means that the beam is in the impulsive regime under the hydrogen explosion. When the structure element is in the impulsive regime under external load, the dynamic amplification factor of this structure is lower than one, which indicates that the dynamic response does not depend on the force peak value (152kPa). This means that it is not so important how the hydrogen pressure varies with time and that the structural response is relative to the explosion impulse.

Figure 6b shows that this given hydrogen explosion pressure stops at 0.024s with a pressure of 89 kPa. Thus, three different overpressure time histories (vertical drop, linear drop with the same slope of the last two data, and nonlinear drop) are simulated in this study to investigate the influence of the pressure impulse.

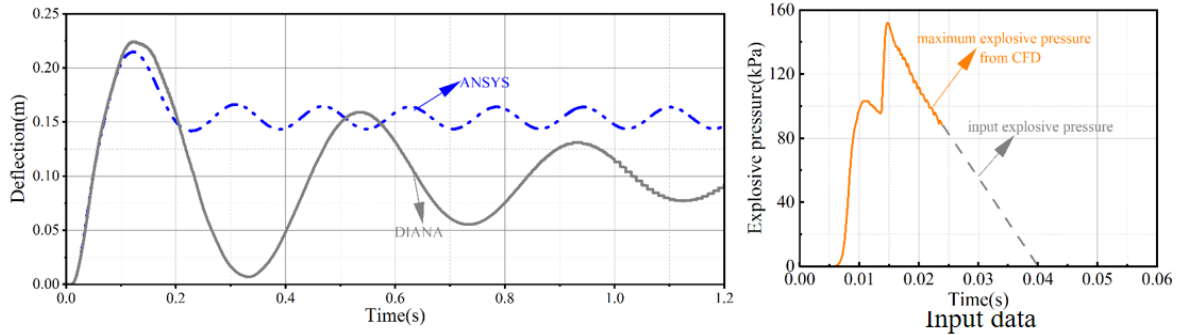
Figure 8 expresses the dynamic displacement response of different pressure waves at the same point (point A) in various software. The dashed line in the input data picture shows the different drop modes, and the solid line is the original hydrogen pressure data from the CFD simulation. The input data in both FE models is the whole line, including the original and drop lines. Regarding the deflection response under different input data, the impulse (area under pressure versus time curve) significantly influences the structure deflection. The larger the impulse value, the higher the slab deflection value.

In Figure 8, the displacement time history is very close between ANSYS and DIANA before the first wave valley in ANSYS arrives. However, the residual deflection of ANSYS is always greater than that value in DIANA. This is attributable to the different concrete material models in the two software. In ANSYS, it is hard to simulate the lower residual strength, and the software can adjust the residual strength based on the convergence, although the input residual strength is very lower. But it is easier to calculate the model with a very low residual strength in DIANA. Therefore, compared with ANSYS Mechanical APDL, DIANA is recommended for use when analysing the nonlinear behaviour of the structure under explosion.

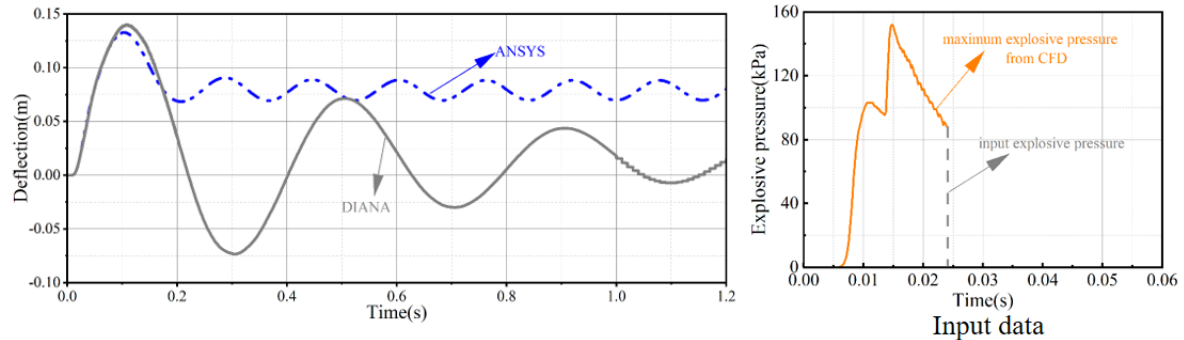
In addition, the time corresponding to the peak displacement value is also delayed, which is larger than the external load duration (0.04s). This also means that a significant delay between the peak of the action and the peak of the response can be expected, as the elastic response of the structure was still growing when the action was ending. Taking Figure 8(b) as an example, the maximum displacement response of the mid-span of the tunnel slab is about 0.225m. Compared with the value in BS 476 [29] and ISO 834-1 [30], it revealed that the displacement is in control, and the slab can resist this explosion pressure without collapsing. However, the smaller residual displacement (0.1m in DIANA and 0.15m in ANSYS) is far from the origin and indicates significant permanent damage. Therefore, the slabs should be retrofitted and reinforced after the explosion to ensure safe use.



(a) Deflection time histories under nonlinear pressure drop



(b) Deflection time histories under linear pressure drop



(c) Deflection time histories under a vertical pressure drop

Figure 8 Deflection time histories of point A on the bottom surface

5. PARAMETRIC ANALYSIS

In this section, parametric studies are carried out to study the effects of reinforcement diameter, reinforcement position, concrete strength, and boundary conditions on the nonlinear performance of an RC ventilation slab in a tunnel with hydrogen explosion loads. Deflection time histories are compared to investigate the RC slab nonlinear behaviour. Furthermore, all of the displacement responses are obtained from two software, ANSYS and DIANA. Three reinforcement diameters (i.e., 12mm, 16mm, 20mm), three reinforcement positions (i.e., 25mm, 40mm, 55mm), and three concrete strengths (i.e., C25, C35, C45) are considered into 9 cases with two software. FE models have the same mesh size and material models for the parametric analysis in chapter 2. The input pressure is selected from the CFD data with a linear drop, see Figure 8(b). All deflection time histories are extracted from the point A on the slab bottom surface, which is the same point as chapter 4.

5.1 Influence of reinforcement

Figure 9 shows the deflection time history of the RC slab with different steel bar diameters. The difference in maximum deflection between the two software increases with the steel bar diameter decrease. Moreover, the smaller the steel bar diameter, the larger the maximum mid-span deflection. For example, when the reinforcement diameter is 12mm, the maximum displacement is 0.315m and 0.29m

in DIANA and ANSYS, respectively, which is larger than 0.175m in DIANA and 0.165m in ANSYS when the bar diameter is 20mm. This phenomenon is caused by the RC slab tensile membrane effect, and the RC slab is easier to collapse when the steel bar diameter is small. Thus, in the case of meeting the design code, using a large-diameter steel bar is suggested in practice engineering.

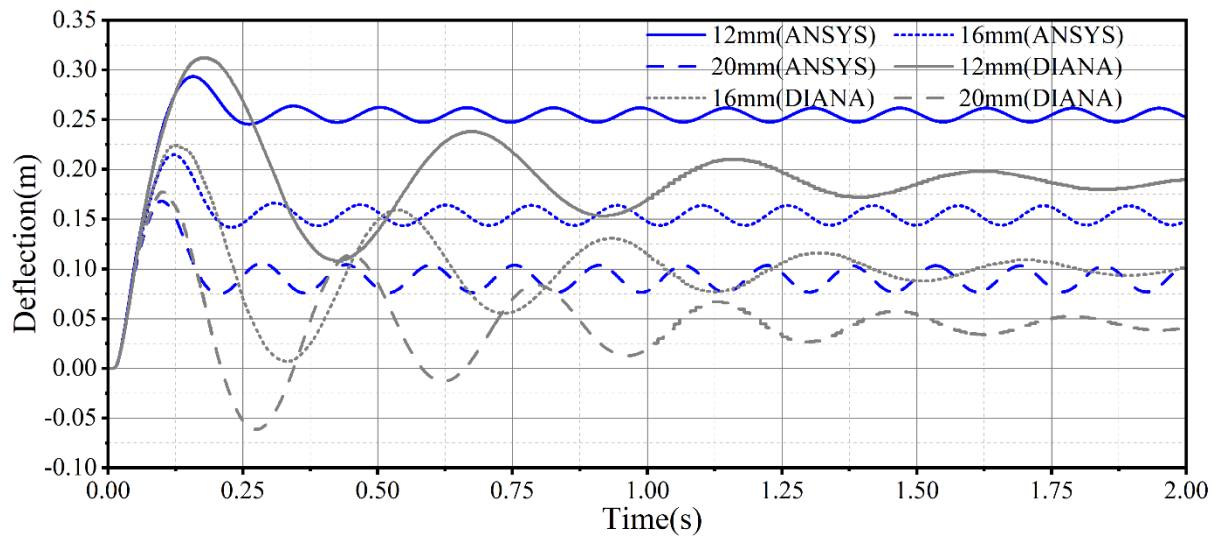


Figure 9 Deflection time history in different reinforcement diameters

5.2 Influence of reinforcement position

The reinforcement position in this section indicates the distance between the concrete surface and the steel bar center, and the beam section size is the same as in chapter 4. The displacement time histories under different reinforcement positions can be seen in Figure 10. The maximum deflection in distinct cases is very close, and the deflection has a little improvement with the distance between the concrete surface and the steel bar center decreasing, which means that the reinforcement position is not the dominant influence factor. Compared with the two software, it can be seen that the residual deflection of ANSYS is higher than that in DIANA. Both the residual deflection in ANSYS and DIANA exceed 0.1m. Thus, the RC slab is damaged under this type of hydrogen explosion load, and this damage to the slab is permanent.

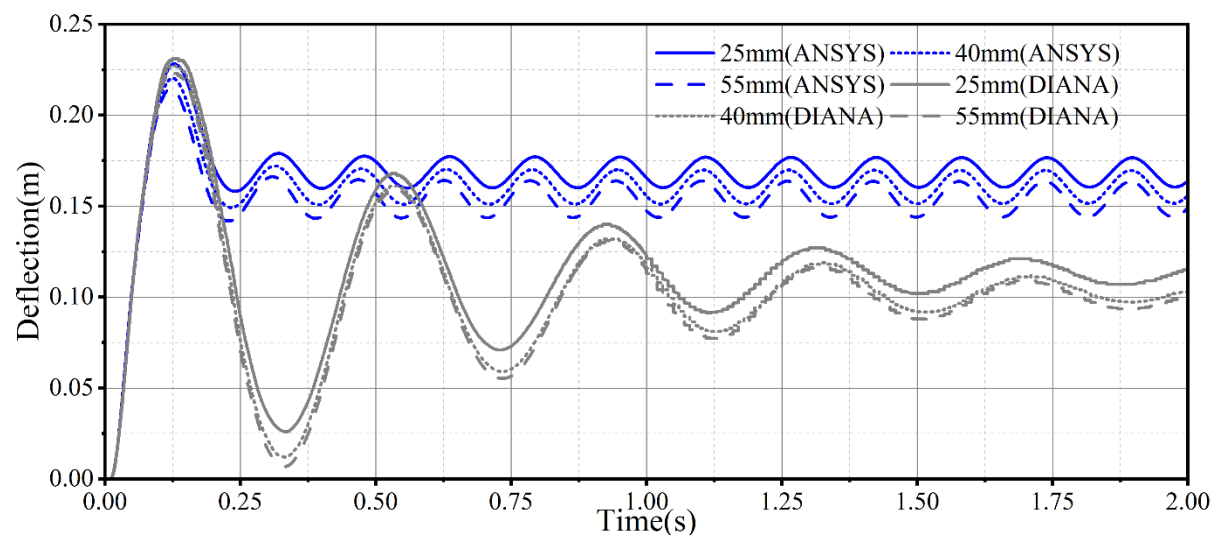


Figure 10 Deflection time history in different reinforcement positions

5.3 Influence of concrete strength

According to Figure 11, the deflection time histories curves for different concrete strengths almost overlapped with each other in the same software. For example, the maximum displacement is around 0.225m in DIANA, although the concrete grade changes from C25 to C45. Furthermore, the maximum deflection has a little discrepancy with concrete strength in ANSYS, from 0.21m to 0.219m. hence, it can be concluded that the influence of concrete strength on the middle point deflection of the RC slab is minor.

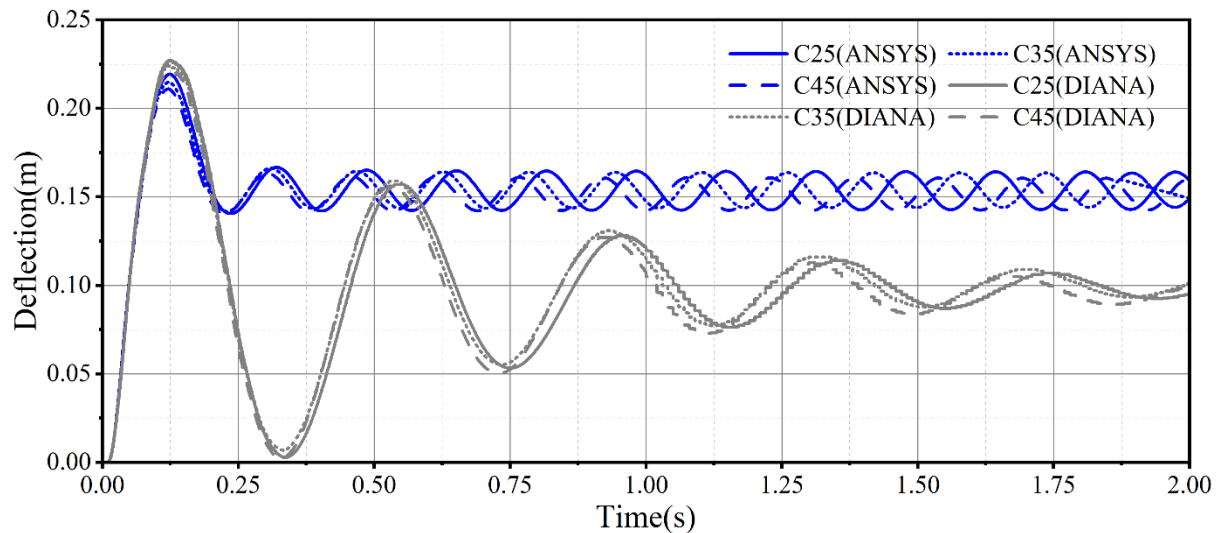


Figure 11 Deflection time history in different concrete strengths

5.4 Influence of boundary condition

In real engineering applications, the boundary of an RC ventilation slab in the tunnel depends on the construction technology. Thus, there are many kinds of boundary conditions for the RC slab. Herein, four different boundary conditions are discussed in this section, as shown in Figure 12. In Figure 12, support 1 indicates that the node is constrained in a vertical and horizontal direction, and support 2 demonstrates that the node is constrained in a vertical direction.

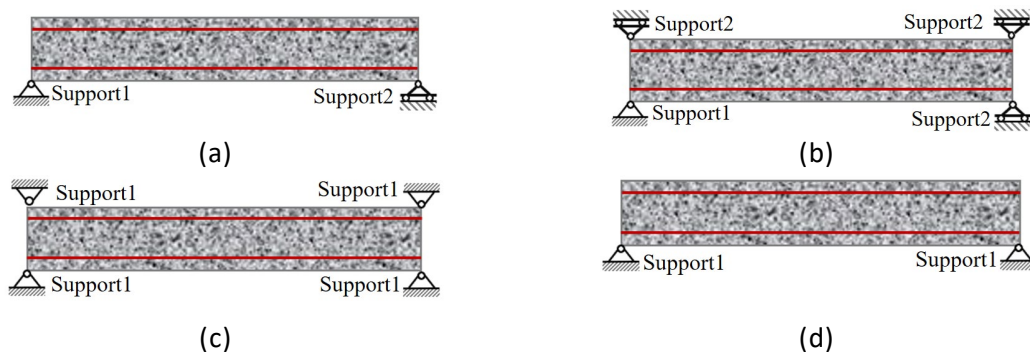


Figure 12 Diagram of RC beam with different boundaries

RC slab middle point displacement responses under various boundaries are presented in Figure 13. The deflection time histories of boundary (a) and (b) in the same software are almost overlapped. It is because of the similar natural period of the RC slab under boundaries (a) and (b). Depending on the maximum deflection of these four boundary conditions, the RC slab under boundary (a) and (b) has the largest value, followed by boundary (d), and the minimum value is shown in boundary (c). The reason for this phenomenon is that the natural period is different in these boundary conditions. Under boundary (c), the RC slab with less freedom has the smallest natural period and largest stiffness among these boundary conditions, which leads to lower deflection when the external load is the same.

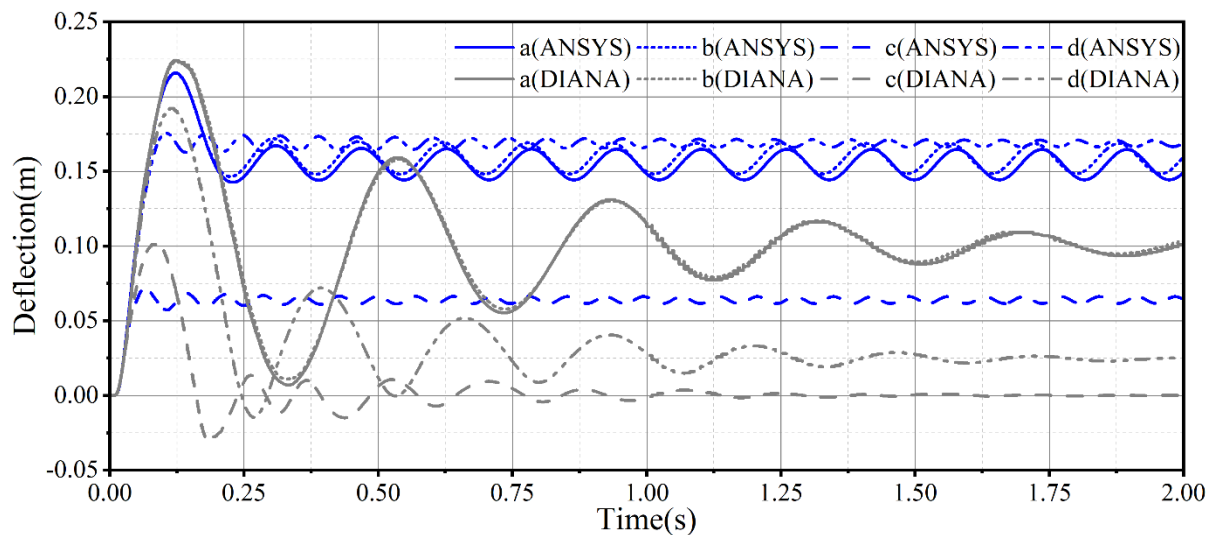


Figure 13 Deflection time history of different boundary conditions in Figure 12

6. CONCLUSION

In this paper, the nonlinear performance of the RC ventilation slab under a hydrogen tank explosion is studied by numerical analysis with two software. The conclusions obtained from this study are summarized as follows:

- (1) The simplified 2D FE models are developed in ANSYS and DIANA, and these FE models are validated by comparing them with experimental data. These numerical models can be used to predict the RC structure deformation under explosions.
- (2) In terms of the RC ventilation slab construction technology, a 2D simplified supported beam can substitute a 3D simplified supported ventilation slab in a tunnel.
- (3) Under a hydrogen tank explosion, the RC ventilation slab deflection is relative to the explosion impulse when the RC slab is in the impulsive regime. And the larger the impulse, the greater the RC slab deflection. Furthermore, slabs should be retrofitted and reinforced after an explosion to ensure safe use when the external impulse is very larger.
- (4) Parametric analysis states that the reinforcement diameter and structure boundary conditions have a significant influence on the structure's dynamic performance. Increasing the reinforcement diameter or reducing the freedom of the structures can reduce structural deformation to some extent. However, the effects of reinforcement position and concrete strength on structural deflection are limited.

ACKNOWLEDGMENT

The authors gratefully acknowledge the financial support provided by the Fuel Cells and Hydrogen 2 Joint Undertaking (now Clean Hydrogen Partnership) under Grant Agreement No 826193. The authors gratefully acknowledge the support from the European Union's Horizon 2020 Research and Innovation program, Hydrogen Europe and Hydrogen Europe Research.

REFERENCES

1. Liu, J., Q. Yan, and J. Wu, *Analysis of blast wave propagation inside tunnel*. Transactions of Tianjin University, 2008. **14**(5): p. 358-362.
2. He, S., et al., *Methane explosion accidents of tunnels in SW China*. Geomatics, Natural Hazards and Risk, 2019. **10**(1): p. 667-677.
3. *Negligence in tunnel collapse that killed 11 workers was covered up: Turkish court of accounts*. 2021: <https://stockholmcf.org/negligence-in-tunnel-collapse-that-killed-11-workers-was-covered-up-turkish-court-of-accounts/>.

4. LaFleur, C.B.B.A., G.A.; Muna, A.B.; Ehrhart, B.D.; Blaylock, M.L.; Houf, W.G., *Hydrogen Fuel Cell Electric Vehicle Tunnel safety study*. 2017, Sandia National Laboratories: Albuquerque, NM, USA. p. 36–71.
5. Robert Zalosh, N.W., *Hydrogen fuel tank fire exposure burst test*. 2005. p. 2338–2343.
6. Glover, A.M.B., A.R.; LaFleur, C.B., *Hydrogen Fuel Cell Vehicles in Tunnels*. 2020, Sandia National Laboratories: Albuquerque, NM, USA. p. 54–59.
7. Groethe, M., et al., *Large-scale hydrogen deflagrations and detonations*. International Journal of Hydrogen Energy, 2007. **32**(13): p. 2125-2133.
8. Li, Y.Z., *Study of fire and explosion hazards of alternative fuel vehicles in tunnels*. Fire Safety Journal, 2019. **110**: p. 102871.
9. Wang, S., et al., *Performance of utility tunnels under gas explosion loads*. Tunnelling and Underground Space Technology, 2021. **109**: p. 103762.
10. Buonsanti, M. and G. Leonardi, *3-D simulation of tunnel structures under blast loading*. Archives of Civil and Mechanical Engineering, 2013. **13**(1): p. 128-134.
11. Li, Z., et al., *Numerical Investigation of the Dynamic Responses and Damage of Linings Subjected to Violent Gas Explosions inside Highway Tunnels*. Shock and Vibration, 2018. **2018**: p. 1-20.
12. Shukla, P.J., A.K. Desai, and C.D. Modhera, *Dynamic response of cut and cover tunnel section under blast loading*. Innovative Infrastructure Solutions, 2020. **6**(1).
13. Koneswaran, S., D.P. Thambiratnam, and C. Gallage, *Blast Response of Segmented Bored Tunnel using Coupled SPH-FE Method*. Structures, 2015. **2**: p. 58-71.
14. Liu, H., *Dynamic Analysis of Subway Structures Under Blast Loading*. Geotechnical and Geological Engineering, 2009. **27**(6): p. 699-711.
15. Sadique, M.R., M. Zaid, and M.M. Alam, *Rock Tunnel Performance Under Blast Loading Through Finite Element Analysis*. Geotechnical and Geological Engineering, 2021. **40**(1): p. 35-56.
16. Cheng, R., et al., *Effect of internal explosion on tunnel secondary and adjacent structures: A review*. Tunnelling and Underground Space Technology, 2022. **126**: p. 104536.
17. https://hytunnel.net/wordpress/wp-content/uploads/2022/09/HyTunnel-CS_D4.3_Final-report-on-analytical-numerical-and-experimental-studies-on-explosions.pdf.
18. I, A., *ANSYS Mechanical APDL Material Reference*. 2022, ANSYS, Inc
19. *DIANA – Finite Element Analysis*, in *DIANA Documentation release 10.4*, D.F.a.J. Manie, Editor., DIANA FEA bv: Netherlands.
20. *DIANA – Finite Element Analysis*, in *DIANA Documentation release 10.4*, D.F.a.J. Manie, Editor. 2022, DIANA FEA bv: Netherlands.
21. Lu, Y. and K. Xu, *Modelling of dynamic behaviour of concrete materials under blast loading*. International Journal of Solids and Structures, 2004. **41**(1): p. 131-143.
22. Holmquist, T.J., Johnson, G.R., Cook, W.H., *A computational constitutive model for concrete subjected to large strains, high strain rates, and high pressures*, in *In: 14th International Symposium on Ballistics*. 1993: Quebec, Canada. p. 591–600.
23. Reinhardt, H.W., Rossi, P., Mier van, J.G.M., *Joint investigation of concrete at high rates of loading*. Materials and Structures, 1990. **23**: p. 213–216.
24. CEB-FIP., *Model code 1990*. Paris: Comite EURO-international du beton. 1991: p. 87-109.
25. Malvar, L.J., Crawford, J.E., *Dynamic Increase Factors for Steel Reinforcing Bars*, in *28th DDESB Seminar*. 1998: Orlando, USA.
26. Rao, B., et al., *Dynamic responses of reinforced concrete beams under double-end-initiated close-in explosion*. Defence Technology, 2018. **14**(5): p. 527-539.
27. Molkov, V.V., et al., *Dynamics of blast wave and fireball after hydrogen tank rupture in a fire in the open atmosphere*. International Journal of Hydrogen Energy, 2021. **46**(5): p. 4644-4665.
28. V. Shentsov, D.M., and V. Molkov. *Blast wave after hydrogen storage tank rupture in a tunnel fire*. in *International Symposium on Tunnel Safety and Security 2018*. Borås, Sweden. 476-10, BS., *Fire tests on building materials and structures. Guide to the principles, selection, role and application of fire testing and their outputs*. 2009.
29. 834-1, ISO., *Fire-resistance tests - Elements of building construction*. 1999.

